Physica B 405 (2010) 4551–4555

Contents lists available at ScienceDirect

Physica B

journal homepage: www.elsevier.com/locate/physb

Quenching of the surface-state-related photoluminescence in Ni-coated ZnO nanowires

Yang Tang [a,b], Dongxu Zhao [a,*], Jiying Zhang [a], Dezhen Shen [a]

[a] Key Laboratory of Excited State Processes, Changchun Institute of Optics, Fine Mechanics and Physics, Chinese Academy of Sciences, 16 East Nan-Hu Road, Open Economic Zone, Changchun 130033, People's Republic of China
[b] Graduate School of the Chinese Academy of Sciences, People's Republic of China

ARTICLE INFO

Article history:
Received 12 October 2009
Received in revised form
2 August 2010
Accepted 12 August 2010

Keywords:
ZnO nanowire
Ni-coated
Electrodeposition
Surface states

ABSTRACT

Nickel-coated ZnO nanowires (NWs) were fabricated by electrodepositing Ni particles on ZnO NW arrays. The morphological, magnetic, and photoluminescent properties of the Ni-coated ZnO NWs were investigated. The Ni particles were deposited on the ZnO NWs' surface along its length to form a Ni/ZnO shell-core structure. The Ni-coated ZnO NWs exhibited more isotropic characteristic than the electrodeposited Ni films owing to the isotropic sphere structure of the Ni particles. A strong ultraviolet emission can be obtained from the Ni-coated ZnO NWs, while the green emission related to surface states was quenched by the passivated layer.

1. Introduction

As a wide band-gap semiconductor, one dimensional ZnO nanostructures have aroused intense theoretical and experimental research interests worldwide in recent years because of their potential applications as ultraviolet lasers [1], field-effect transistors [2], gas sensors [3], field-emission displays [4], and nanogenerators [5,6]. Owing to the large aspect ratio, the luminescence properties of ZnO nanowires (NWs) may degrade as result of the unpassivated surface states serving as the nonradiative recombination centers [7,8]. The surface passivation is adopted to generate desired NW surface characteristics and improve luminescence properties [9]. The optical quenching with increasing temperature have been reported in Ni-nanodot-coated ZnO NWs [10]. As an important transitional metal, Ni has attracted great attention in terms of its expected applications in high-density magnetic recording, magnetic sensors, catalysis, and Ni-based batteries [11–14]. The fabrication of magnetic materials/semiconductor heterostructures is of particular interest in nanoscale spintronics [15]. The Ni-passivated ZnO NWs not only exhibit the improvement of the photoluminescence property by the surface passivation, but also are regarded as a formation of junction, which may serve as a basic unit for the optoelectronic nanodevices.

Electrochemical techniques are particularly attractive for the electrodeposition of metallic nanostructures [16]. In this paper nickel particles were electrodeposited on ZnO NW arrays to form a Ni/ZnO shell-core NW structure. It is expected that the ability to grow magnetic-metal/semiconductor NW heterostructures can improve the luminescence properties by surface passivation and increase versatility and power of these building blocks for applications in nanoscale spintronics and optical nanodevices [15]. In addition, magnetic fields have been used to control the direction and the position of magnetic nanowires and Ni end-capped nonmagnetic nanowires recently [17–19]. Therefore, it is expected that the Ni-coated ZnO NWs can be applied to make a matrix of devices as well as a single device using magnetic alignment.

2. Experimental methods

Our study is based on the aligned ZnO NWs arrays grown on p-Si (1 0 0) substrate by vapor transport process. The silicon substrate was pre-coated with a ZnO thin layer. The details of the NW growth were concluded in Refs. [20,21]. After the fabrication of ZnO nanowires arrays, the wafers were then transferred to the electrodeposition cell with aqueous electrolytes containing 0.01 M $Ni(CH_3COO)_2$ as the source of metal ions and 0.05 M CH_3COONH_4 as the supporting electrolyte. A Pt counter electrode and an Ag/AgCl reference electrode were adapted. The electrodeposition was carried out at a constant potential of −1950 mV at room temperature. The growth time was held for 10 min. The surface morphology of the nanostructures was observed by field emission scanning electron

* Corresponding author. Tel.: +86 431 86176322; fax: +86 431 84627031.
E-mail address: dxzhao2000@yahoo.com.cn (D. Zhao).

0921-4526/$ - see front matter © 2010 Elsevier B.V. All rights reserved.
doi:10.1016/j.physb.2010.08.036

microscopy (FESEM, Hitachi S-4800) and energy-dispersive X-ray (EDX) attached to the SEM. Magnetic characteristics were studied using a vibrating sample magnetometer (VSM) (Lake Shore Company) at room temperature. Micro-PL spectra were measured using the 325 nm line of a He–Cd laser as an excitation source.

3. Results and discussion

When Ni was electrodeposited directly on silicon, uniform Ni thin films can be obtained. The substrate surface is entirely covered by the compact Ni films. The details of the Ni films electrodeposited on silicon were concluded in Ref. [22]. The ZnO NWs grown on the silicon substrate form a matrix, indicated in Fig. 1(a). The ZnO NW has a typical diameter of 70 nm and the length of 4 μm. After the Ni electrodeposition for 10 min, there were great changes in morphology. Ni particles can be observed on the top and lateral surface of ZnO NWs as shown in Fig. 1(b). The previous smooth ZnO NW surfaces became rough owing to the electrodeposited Ni particles. The Ni-coated ZnO NW arrays turned out to be bundled together under the capillary force. The bundling behavior of ZnO NWs by capillary force was included in our previous report [23]. There were two kinds of Ni particles on ZnO NW arrays. At first, the Ni particles were deposited on the ZnO NW surfaces along its length to form a Ni/ZnO shell-core structure. When the ZnO NWs were bundled together under the capillary force, the Ni started to deposit on the top area of the ZnO NW bundles. As a result, the Ni micro-particle blocks formed as shown in Fig. 1(c). The inset image of Fig. 1(c) illustrates that the block is consisted of compact Ni grains. There were no Ni micro particles on the bundles that included less ZnO NWs in Fig. 1(d). The ZnO NW bundles composed of a certain quantity of NWs acted as the nucleation sites for the following growth of Ni micro-particle blocks. For the shell-core structure in Fig. 2(a), the ZnO NW was entirely covered by the string bead-like Ni nanoparticles. The boundary between the adjacent Ni particles was obvious in Fig. 2(b). At the top area of ZnO NW, the density of the Ni particles was larger, which is depicted in Fig. 2(c). The circle area in Fig. 2(c) indicates that some ZnO NWs could break as a result of the capillary force. According to Fig. 2(d), the electrodeposited Ni particle has a typical diameter of 260 nm. The ZnO NWs in the electrodeposition process could be viewed as nano-electrode arrays. The electrodeposition process is a complex multi-step procedure. The changes in the electrolyte bulk phase and the electrode interface are continuous during the deposition process. In our previous report NH_4^+ ions in the electrolyte play a role to assist the Ni deposition [22]. The Ni^{2+} and its ammonium group complex in the electrolytes transfer to the vicinity of the electrode interface. The ions discharge at the interface, then generate the absorbed atoms. The Ni electrodeposition process in the electrolyte is as follows [24]:

$$[Ni(NH_3)_2]^{2+} = Ni^{2+} + 2NH_3 \quad (1)$$

$$Ni^{2+} + 2e \rightarrow Ni \quad (2)$$

A negative potential (-1.95 V) makes the reactions go along the path (1)→(2), which results in the growth of the Ni particles over the whole surface of the ZnO NWs.

Fig. 3(a) shows the EDS result of the as-synthesized ZnO NWs. In addition to the Si signal from the substrate, there were only Zn and O signals. After the Ni electrodeposition, the Ni signals were obvious in Fig. 3(b). No other signals except for Zn, O, and Ni were observed.

Fig. 4 shows the room temperature hysteresis loops of Ni-coated ZnO NWs while the applied magnetic field is parallel and perpendicular to the sample surface. The coercive force and remanence ratio were 93 Oe and 15% while the magnetic field was parallel to the sample surface and 74 Oe and 9.2% while the applied field perpendicular to the surface. Both coercive forces were smaller than that of Ni bulk materials (100 Oe) but the remanences were larger than that of the bulk Ni (4.9%) [25]. The magnetic properties of nanomaterials are dependent on the shape, crystallinity, magnetization directions, and so on [26]. Because Ni exhibits a small magnetocrystalline anisotropy, the magnetic response is expected to be dominated by the shape anisotropy. It was reported that electrodeposited Ni films had strong shape anisotropy exhibiting characteristic of easy

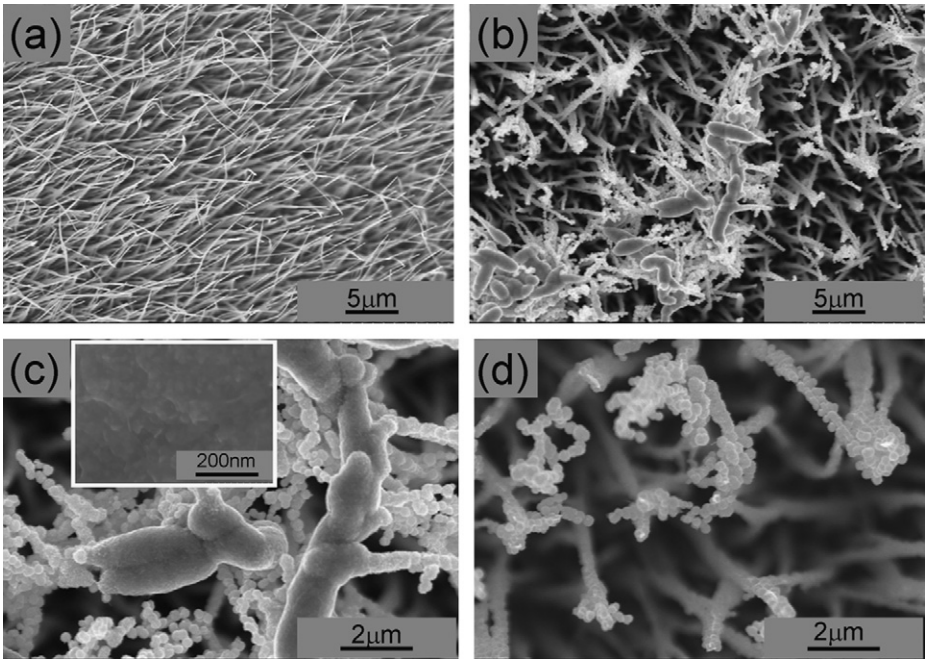

Fig. 1. (a) SEM images of the as-synthesized ZnO NW arrays; (b), (c), and (d) SEM images of the Ni/ZnO shell-core NWs. Inset image of (c): an enlarged view of the Ni micro-particle block.

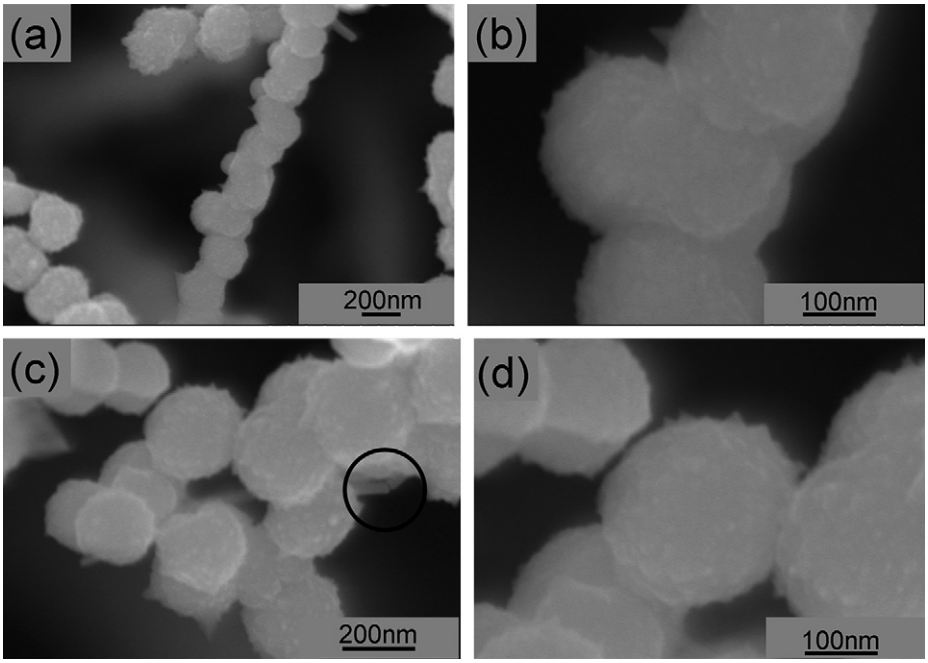

Fig. 2. SEM images of the Ni-coated ZnO NWs.

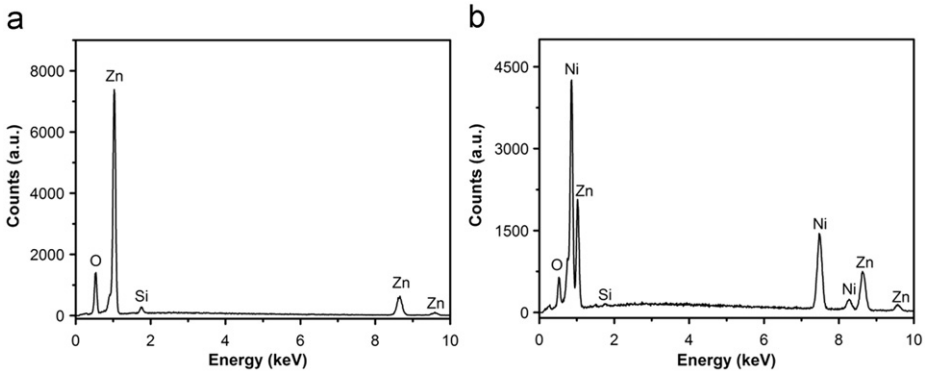

Fig. 3. EDS spectrum of (a) the as-synthesized ZnO NW arrays and (b) the Ni-coated ZnO NWs.

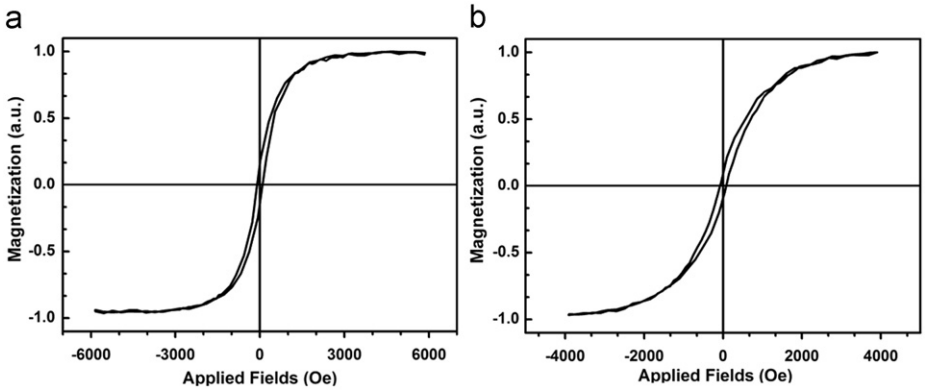

Fig. 4. VSM hysteresis loop of the Ni-coated ZnO NWs. The magnetic field was applied parallel (a) and perpendicular (b) to the substrate surface.

magnetized axis (Mr/Ms=0.67) while the applied magnetic field was parallel to the film plane and the characteristic of hard magnetized axis (smaller than 0.02) while the applied field was perpendicular to the film plane [27]. However, the Ni/ZnO shell-core NWs in this paper exhibited more isotropic characteristic (much smaller contrast of the remanences under parallel and perpendicular magnetic fields) than the electrodeposited Ni films. It is attributed to the isotropic sphere structure of the Ni particles electrodeposited on ZnO NWs. The more isotropic behavior in the magnetic response was observed in Ni hollow sphere arrays [28].

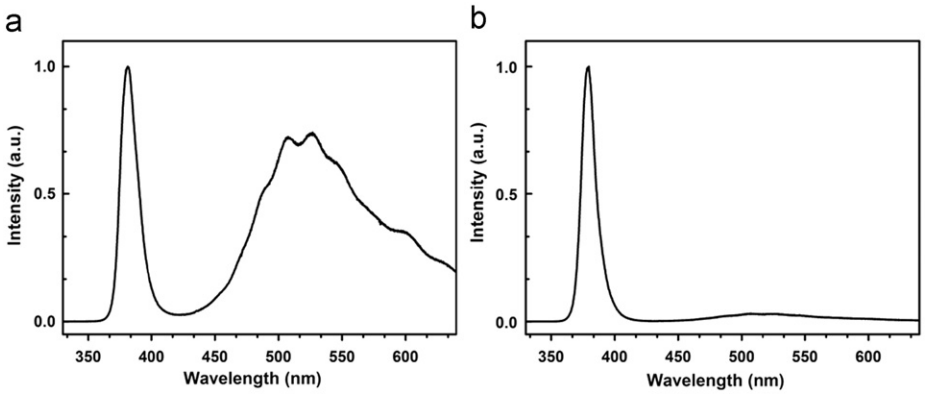

Fig. 5. Room temperature photoluminescence spectrum of (a) the as-synthesized ZnO NW arrays (b) the Ni-coated ZnO NWs.

Jung et al. [15] evaporated Ni on the tips of ZnO nanorods and investigated the structural and magnetic properties of the heterostructure. However, it was not possible for the Ni particles to cover the whole surface of the ZnO nanorods using the evaporation method. An alternative way is to treat the NiO-coated ZnO NWs by thermal annealing with the H_2 reduction process [10]. With the thermal-reduction process, NiO changed to Ni nanodot. However, there were some space between the Ni nanodots and the atomic layer deposition (ALD) process was essential for coating NiO on ZnO NWs. Our results by electrochemical deposition take advantages of the low cost, the low-temperature process, the possibility in preparing large scale materials, and the complete coating on the NWs' surface. As a low-temperature process, the electrodeposition can avoid interdiffusion and compound formation at the interfaces so that an abrupt and clean interface could be created, which is necessary for the injection of spin-polarized currents from the ferromagnet to the semiconductor [29].

Photoluminescence (PL) measurements of the Ni-coated ZnO NWs were conducted under excitation of a 325 nm He–Cd laser at room temperature. As shown in Fig. 5(a), the PL spectrum of the as-synthesized ZnO NWs shows a strong ultraviolet emission line from ZnO-free exciton and a negligibly weak green emission band around 525 nm. The intensity ratio of the UV emission and the visible emission of the as-synthesized ZnO NWs is 1.35. After the electrodeposition of Ni on ZnO NW arrays, a great decrease of deep level emission in the PL spectrum of the Ni-coated ZnO NWs is illustrated in Fig. 5(b). The intensity ratio of the UV emission and the visible emission of the Ni/ZnO shell-core NWs is 32, which is almost 24 times larger than that of the as-synthesized ZnO NWs. All spectra were obtained in one session under an identical excitation and collection conditions. Because the as-synthesized ZnO NWs has a large aspect ratio, the surface approaches the bulk and the luminescence properties of ZnO NWs are dominated by properties of surfaces. Within an effective distance from the surface the excited carriers would diffuse to the surface and recombine at the surface defects [30]. Therefore, the visible emission in the as-synthesized ZnO NWs mostly originates from surface states owing to their relatively large aspect ratio. In addition, van Dijken et al. [31] also proposed a kind of mechanism for the visible green emission. That is, the photogenerated hole was trapped by surface states or defects (probably O^{2-}/O^{-}). The surface trapped hole tunneled back into the bulk volume, where it recombined with an electron to form the Vo^{**} center. Finally, the green emission was assigned to the recombination of a shallowly trapped electron with a deeply trapped hole in a Vo^{**} center. After the electrodeposition of Ni, an interface between the Ni shell and the ZnO NW core formed, which greatly passivated the surface states of the ZnO NWs. The excited carriers that diffuse to the surface were quenched by passivated layer. Otherwise, it is impossible for the trapped hole by the surface states tunnels back to bulk volume to form Vo^{**} center. According to the mechanism of visible emission and the model of a core-shell structure for the Ni/ZnO shell-core NWs, a strong ultraviolet emission from the Ni/ZnO shell-core NWs was expected, while the green emission would be quenched, which agrees with the PL result.

4. Conclusions

In conclusion, a structure of Ni-coated ZnO NWs was fabricated by electrodepositing Ni particles on ZnO NW arrays. The Ni particles were deposited on the ZnO NW surfaces along its length to form a Ni/ZnO shell-core structure. The Ni/ZnO shell-core NWs exhibited more isotropic characteristic than the electrodeposited Ni films owing to the isotropic sphere structure of the Ni particles. The Ni-coated ZnO NWs showed a strong ultraviolet emission, while the green emission related to surface states was quenched by the passivated layer. The improvement of the Ni-coated ZnO NWs in optical quality is expected to combine the merits of both high quality ZnO NWs and magnetic Ni particles. They could exhibit some new physical properties and stimulate further investigations. For example, the Ni/ZnO shell-core structure, which is a radial structure, namely nanocables, can provide a more efficient injection current with respect to the crossed and the axial structures [32,33]. The magnetic-semiconductor nanowire structures might be used as components for nanoscale spin-valve transistors, spin light-emitting diodes, nonvolatile storage, and logic devices [15]. In addition, the magnetic Ni/ZnO structure could be controlled to build a matrix of nanodevices using magnetic alignment. Therefore it is expected that the ability to grow magnetic Ni/ZnO NW structure can improve the luminescence properties by surface passivation and increase versatility and power of these building blocks for applications in nanoscale spintronics or optical nanodevices.

Acknowledgements

This work was supported by the Key Project of National Natural Science Foundation of China under Grant nos. 60336020 and 50532050, the "973" Program under Grant no. 2006CB604906, the CAS Innovation Program, the National Natural Science Foundation of China under Grant nos. 60429403, 60506014, 50402016, and 10674133.

References

[1] M.H. Huang, S. Mao, H. Feick, H. Yan, Y. Wu, H. Kind, E. Weber, R. Russo, P. Yang, Science 292 (2001) 1897.
[2] X. Wang, J. Zhou, J. Song, J. Liu, N. Xu, Z.L. Wang, Nano Lett. 6 (2006) 2768.
[3] M.S. Arnold, P. Avouris, Z.W. Pan, Z.L. Wang, J. Phys. Chem. B 107 (2003) 659.
[4] C.J. Lee, T.J. Lee, S.C. Lyu, Y. Zhang, H. Ruh, H.J. Lee, Appl. Phys. Lett. 81 (2002) 3648.
[5] Z.L. Wang, J. Song, Science 312 (2006) 242.
[6] X. Wang, J. Song, J. Liu, Z.L. Wang, Science 316 (2007) 102.
[7] B.D. Yao, Y.F. Chan, N. Wang, Appl. Phys. Lett. 81 (2002) 757.
[8] J.W. Chiou, K.P. Krishna Kumar, J.C. Jan, H.M. Tsai, C.W. Bao, W.F. Pong, F.Z. Chien, M.-H. Tsai, I.-H. Hong, R. Klauser, J.F. Lee, J.J. Wu, S.C. Liu, Appl. Phys. Lett. 85 (2004) 3220.
[9] L. Shi, Y. Xu, S. Hark, Y. Liu, S. Wang, L. Peng, K. Wong, Q. Li, Nano Lett. 7 (2007) 3559.
[10] Y.H. Park, Y.H. Shin, S.J. Noh, Y. Kim, S.S. Lee, C.G. Kim, K.S. An, C.Y. Park, Appl. Phys. Lett. 91 (2007) 012102.
[11] Q. Liu, H. Liu, M. Han, J. Zhu, Y. Liang, Z. Xu, Y. Song, Adv. Mater. 17 (2005) 1995.
[12] P. Jin, Q. Chen, L. Hao, R. Tian, L. Zhang, L. Wang, J. Phys. Chem. B 108 (2004) 6311.
[13] D. Wang, C. Song, Z. Hu, X. Fu, J. Phys. Chem. B 109 (2005) 1125.
[14] J. Bao, Y. Liang, Z. Xu, L. Si, Adv. Mater. 15 (2003) 1832.
[15] S.W. Jung, W.I. Park, G.–C. Yi, M.Y. Kim, Adv. Mater. 15 (2003) 1358.
[16] R.M. Penner, J. Phys. Chem. B 106 (2002) 3339.
[17] M. Tanase, D.M. Silevitch, A. Hultgren, L.A. Bauer, P.C. Searson, G.J. Meyer, D.H. Reich, J. Appl. Phys. 91 (2002) 8549.
[18] A.K. Bentley, J.S. Trethewey, A.B. Ellis, W.C. Crone, Nano Lett. 4 (2004) 487.
[19] S.-W. Lee, M.-C. Jeong, J.-M. Myoung, G.-S. Chae, I.-J. Chung, Appl. Phys. Lett. 90 (2007) 133115.
[20] D. Zhao, C. Andreazza, P. Andreazza, J. Ma, Y. Liu, D. Shen, Chem. Phys. Lett. 408 (2005) 335.
[21] F. Fang, D.X. Zhao, J.Y. Zhang, D.Z. Shen, Y.M. Lu, X.W. Fan, B.H. Li, X.H. Wang, Nanotechnology 18 (2007) 235604.
[22] Y. Tang, D. Zhao, D. Shen, J. Zhang, B. Li, Y. Lu, X. Fan, Thin Solid Films 516 (2008) 2094.
[23] Y. Tang, D. Zhao, J. Chen, N. Wanderka, D. Shen, F. Fang, Z. Guo, J. Zhang, X. Wang, Mater. Chem. Phys. 121 (2010) 541.
[24] G. Duan, W. Cai, Y. Luo, Z. Li, Y. Lei, J. Phys. Chem. B 110 (2006) 15729.
[25] J.-H. Hwang, V.P. Dravid, M.H. Teng, J.J. Host, B.R. Elliott, D.L. Johnson, T.O. Mason, J. Mater. Res. 12 (1997) 1076.
[26] Z. Liu, S. Li, Y. Yang, S. Peng, Z. Hu, Y. Qian, Adv. Mater. 15 (2003) 1946.
[27] T.S. Eagleton, P.C. Searson, Chem. Mater. 16 (2004) 5027.
[28] G. Duan, W. Cai, Y. Li, Z. Li, B. Cao, Y. Luo, J. Phys. Chem. B 110 (2006) 7184.
[29] P. Evans, C. Scheck, R. Schad, G. Zangari, J. Magn. Magn. Mater. 260 (2003) 467.
[30] I. Shalish, H. Temkin, V. Narayanamurti, Phys. Rev. B 69 (2004) 245401.
[31] A. van Dijken, E.A. Meulenkamp, D. Vanmaekelbergh, A. Meijerink, J. Phys. Chem. B 104 (2000) 1715.
[32] T. Fukumura, Z. Jin, A. Ohtomo, H. Koinuma, M. Kawasaki, Appl. Phys. Lett. 75 (1999) 3366.
[33] D. Wang, S. Park, Y. Lee, T. Eom, S. Lee, Y. Lee, C. Choi, J. Li, C. Liu, Cryst. Growth Des. 9 (2009) 2124.